ATMOSPHERIC SCIENCE LETTERS
Atmos. Sci. Let. (2014)
Published online in Wiley Online Library
(wileyonlinelibrary.com) **DOI:** 10.1002/asl2.521

Inhomogeneous influence of the Atlantic warm pool on United States precipitation

Hailong Liu,[1,2]* Chunzai Wang,[2] Sang-Ki Lee[1,2] and David Enfield[1,2]

[1] *Cooperative Institute for Marine and Atmospheric Studies, University of Miami, FL, USA*
[2] *Atlantic Oceanographic and Meteorological Laboratory, NOAA, Miami, FL, USA*

**Correspondence to: H. Liu, Cooperative Institute for Marine and Atmospheric Studies, University of Miami, 4600 Rickenbacker Causeway, Miami, FL 33149, USA. E-mail: hliu@rsmas.miami.edu*

Received: 7 April 2014
Revised: 15 July 2014
Accepted: 16 July 2014

Abstract

On interannual time scales, the warming of the Atlantic warm pool (AWP) is associated with a tripole sea surface temperature (SST) pattern in the North Atlantic and leads to more rainfall in the central and eastern US. On decadal-to-multidecadal time scales, the AWP warming corresponds to a basin-wide warming pattern and results in less precipitation in the central and eastern US. The inhomogeneous relationship between the AWP warming and US rainfall on different time scales is largely due to the sign of mid-latitude SST anomaly. The negative mid-latitude SST anomaly associated with the tripole pattern may enhance the low sea level pressure over the northeastern North American continent and also enhance the barotropic response there of the AWP-induced barotropic Rossby wave. This strengthened low pressure system, which is not exhibited when the warming is basin-wide, results in a different moisture transport variation and thus the rainfall pattern over the United States.

Keywords: **climate variability; US precipitation; midlatitude air–sea interaction**

1. Introduction

Understanding the mechanisms of precipitation variability is necessary to improve the reliability of extreme hydroclimate event prediction and thus to alleviate the social and ecological hazards ensued. How the sea surface temperature (SST) of the Pacific and/or the Atlantic influences the contiguous United states (hereinafter abbreviated as US in this context) precipitation has been extensively studied (Ting and Wang, 1997; Enfield *et al.*, 2001; McCabe *et al.*, 2004; Schubert *et al.*, 2004a, 2004b; Seager *et al.*, 2005; Sutton and Hodson, 2005, 2007; Wang *et al.*, 2006, 2008a; Mo *et al.*, 2009; Kushnir *et al.*, 2010; Ruiz-Barradas and Nigam, 2010; Hu *et al.*, 2011; Li *et al.*, 2011; Nigam *et al.*, 2011; Dai, 2013; Hu and Feng, 2012; Veres and Hu, 2013; Zhu *et al.*, 2013). On interannual time scales, El Niño–Southern Oscillation (ENSO) dominates the winter precipitation variability of North America (Ropelewski and Halpert, 1986; Ting and Wang, 1997; Mo *et al.*, 2009). Both the Arctic Oscillation (AO) and the North Atlantic Oscillation (NAO) also exert forcing on the interannual variation of US precipitation. These interannual forcings primarily modulate the latitudinal position and strength of the mid-latitude westerly jet, lead to low-level divergence or convergence through the westerly jet associated atmospheric circulation, and thus impact on US precipitation (Mo *et al.*, 1995; Trenberth and Guillemot, 1996; Hu and Feng, 2012).

On decadal to multidecadal time scales, the Pacific Decadal Oscillation (PDO) (Mantua *et al.*, 1997) and Atlantic Multidecadal Oscillation (AMO) (Mestas-Nunez and Enfield, 1999) are two major drivers of US precipitation variability (e.g. Enfield *et al.*, 2001; McCabe *et al.*, 2004). McCabe *et al.* (2004) showed that over half (52%) of the spatial and temporal variance in multidecadal drought frequency over the US could be ascribed to the PDO and the AMO. Dai (2013) suggested that decadal precipitation variations over much of the West and Central US are significantly correlated with the evolution of the PDO. The Atlantic SSTs, however, are more often influential in driving multi-year droughts than the Pacific SSTs (Nigam *et al.*, 2011). The Atlantic basin-scale SST anomalies associated the AMO have utmost influence on North American precipitation during boreal summer (Sutton and Hodson, 2005, 2007). As suggested by Enfield *et al.* (2001), the rainfall in the majority US is less than the normal during positive AMO phase. The associated mechanism is that during the warm phase of the AMO, an anomalous three-cell circulation pattern is excited over the North American continent and results in anomalous low-level northerly flow from the Great Plains into the Gulf of Mexico, which inhibits rainfall development (Hu *et al.*, 2011). This process in the positive AMO phase actually corresponds to a frequency increase of large Atlantic warm pools (AWPs) and mitigation in southerly transport of water vapor from the intra-Americas sea (IAS) across the Gulf coast (Wang *et al.*, 2008a, 2008b). Kushnir *et al.* (2010) also pinpointed the cause of the anomalous southward flow over the US and northern Mexico which results in a decreased precipitation there than the warmer-than-normal tropical North Atlantic (TNA).

Nevertheless, Sutton and Hodson (2007) suggested that both tropical and higher-latitude SST anomalies have influenced extratropical climate. The direct response to the extratropical SST anomalies, which have been discussed in Palmer and Sun (1985), Peng and Whitaker (1999) and Kushnir *et al.* (2002), is strongest in June to August (JJA) and can be strengthened by the tropical Atlantic SST anomalies. Although we know the role of a warm tropical Atlantic, if and how the mid-latitude SST anomalies affect the climate response of the tropical SST is still largely unknown. In this analysis delved from observations (data and methods are described in Section 2), we first associate the AWP warming of late summer and early fall with two patterns of the North Atlantic (NA) SST anomalies on different time scales and examine the resulting two precipitation patterns over the US (Section 3). Then, we propose the related physical mechanisms and indicate the role of SST anomaly in the mid-latitude (Section 4). Conclusions and discussion are given in Section 5.

2. Data and methods

We use the SST data from the NOAA (National Oceanic and Atmospheric Administration) Extended Reconstruction Sea Surface Temperature version 3 (ERSSTv3) (Smith *et al.*, 2008). The temporal coverage is from January 1854 to the present. These data can be obtained online (http://www.ncdc.noaa.gov/oa/climate/research/sst/ersstv3.php). Three gridded monthly precipitation datasets are included for comparison and verification of this study's conclusions. The Observed Land Surface Precipitation (OLSP) dataset (Dai *et al.*, 1997) based on gauge records provides the monthly precipitation data from 1850 to 1995. Merged Statistical Analyses of Historical Monthly Precipitation Anomalies (MSAHMPA) dataset resolves interannual and longer time scales and spatial scales larger than 5° over both land and oceans from 1900 to 2000 and is used for climate monitoring, for statistical climate studies of the 20th century, and for helping to evaluate dynamic climate models (Smith *et al.*, 2010). The third monthly precipitation data is from NOAA/Cooperative Institute for Research in Environmental Sciences (CIRES) Twentieth Century Global Reanalysis (20CR) version II (Compo *et al.*, 2011). This atmospheric reanalysis spans the entire 20th century (1871–2008), assimilating only surface observations of synoptic pressure, monthly SST and sea ice distribution. More information about this dataset is provided online (http://www.esrl.noaa.gov/psd/data/20thC_Rean/). The sea level pressure (SLP), geopotential height (HGT), winds and specific humidity from 20CR are also used for mechanism analysis.

The AWP SST index (AWPTI) is defined as the box-averaged SST from the American coast to 40°W and from 5° to 30°N. The interannual band (IB) for the AWPTI is defined as 2–7 years and decadal to multidecadal band (DMB) is longer than 7 years. Moisture transport is integrated from the sea surface to 300 mb. Several statistical approaches widely used in climate data analysis are taken in this study, which include linear regression, moving average filter and empirical orthogonal function (EOF) analysis.

3. The role of the AWP in US precipitation

3.1. AWP variability

The AWP peaks in August to October (ASO) (Wang and Enfield, 2001) and has strong interannual and longer time-scale variations (Wang *et al.*, 2008a, 2008b; Liu *et al.*, 2012). In order to evaluate the AWP variability in ASO, we calculate the AWPTI and decompose the index into the IB and DMB. This is compared with the EOF decomposition of the NA SST data in Figure 1(a) and (b). The DMB AWPTI from 1900 to 2000 shows a positive phase between 1930 and 1960 and two negative phases respectively before 1930 and after 1960. Its variation is within −2 to 2 °C (Figure 1(a)), and the phase of the DMB AWPTI coincides with the cycle of the AMO (Wang *et al.*, 2008b). On interannual time scales, the IB AWPTI exhibits strong year-to-year variability within the range of −2.5 to 2.5 °C (Figure 1(b)).

The spatial patterns of NA SST associated with AWPTI on different time scales are further examined. The regression of the NA SST onto DMB AWPTI shows that the whole basin of the NA is in the same phase with the maximum center between 30° and 60°N (Figure 1(e)), suggesting that the warming of the AWP on decadal-to-multidecadal time scales corresponds to the warming of the entire NA basin which is a distinguishing feature of the AMO (Enfield *et al.*, 2001). Regression of the NA SST in ASO onto IB AWPTI produces a tripole pattern (Figure 1(f)). Compared with the winter tripole pattern which has centers east of Newfoundland, near the southeastern coast of the US, and in the tropical eastern Atlantic (Kushnir, 1994; Fan and Schneider, 2012), this ASO tripole pattern moves southward with two maximum centers located in the TNA to the south of 30°N and in the subpolar region to the north of 50°N. The negative center is to the east of the American continent coast between 30° and 50°N. This tripole pattern suggests that the warming of the AWP on interannual time scales corresponds to the warming in both the TNA and subpolar region and cooling in the NA mid-latitudes.

The two NA patterns associated with the AWP warming discussed above are also the first two EOF modes of NA variability in ASO. The first mode with 27.3% variance shows the AMO signature and resembles the regression pattern of the NA SST on the DMB AWPTI (Figure 1(c)). The PC1 time series has a significant correlation with DMB AWPTI with a correlation coefficient of 0.69 (Figure 1(a)). This confirms that the ASO AWP variability on decadal-to-multidecadal scales is a reflection of the AMO (Wang *et al.*, 2008b). The second EOF mode with variance of 13.0% shows a tripole

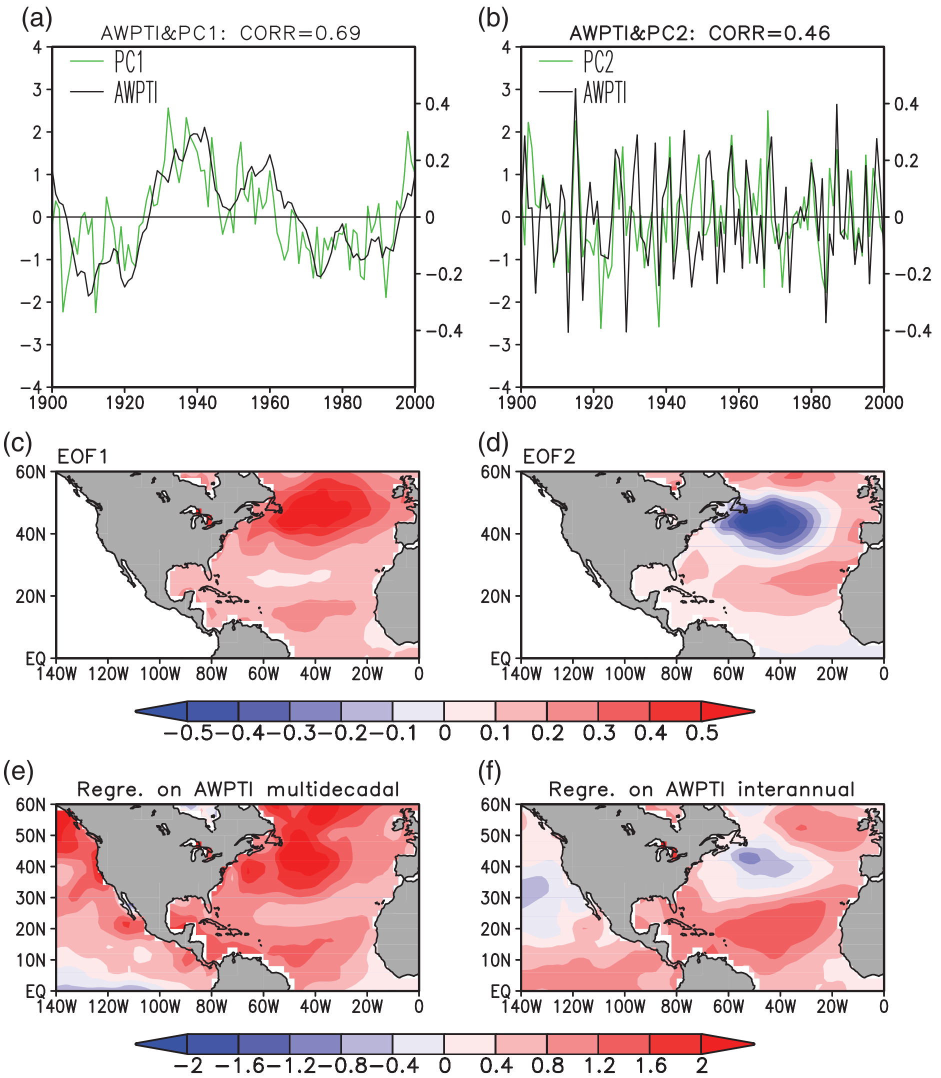

Figure 1. (a) Time series of ASO AWPTI at decadal to multidecadal time scales and principal component of the first EOF mode of the North Atlantic in ASO. (b) Time series of ASO AWPTI at decadal to interannual time scales and principal component of the second EOF mode of the North Atlantic in ASO. (c) The first mode and (d) second mode of the EOF analysis of the North Atlantic SST in ASO. Regression of the North Atlantic SST on AWPTI (e) at decadal to multidecadal time scales and (f) at interannual time scales.

pattern (Figure 1(d)) that shares the similarity with the pattern of regression of the NA SST onto IB AWPTI. The PC2 and the IB AWPTI are also significantly correlated with the correlation coefficient of 0.46. Thus, it can be concluded that the interannual variability of the ASO AWP is closely related with the tripole mode of the NA.

3.2. The impact of AWP on US precipitation in ASO

Wang *et al.* (2008a) suggested that an anomalously large AWP decreases the summer rainfall over the central US based on model experiments forced by the SST composites of six large warm pool years. They also pointed out that roughly 80% of large and small AWPs occur in the warm and cool phases of the AMO, suggesting that the impact of the AMO on US precipitation is largely through the impact of warm pool variability on circulation patterns and moisture transport. In order to evaluate the roles of the AWP on different time scales, we perform the regression of ASO precipitation onto AWPTI filtered for IB and DMB (Figure 2). For the OLSP station rainfall dataset, the regression onto IB AWPTI shows that with a demarcation line at 100°W, a warm AWP is interannually associated with more precipitation in the central and the eastern US and less precipitation in the western US. This pattern is also well represented in Figure 2(c) based on the 20CR dataset. For the MSAHMPA dataset (Figure 2(e)), the pattern of more precipitation in the central and eastern US is consistent with the patterns of the OLSP and 20CR dataset. But in the western US the dry pattern of Figure 2(a) and (c) is not captured in the MSAHMPA dataset, which may be caused by the coarse resolution of the MSAHMPA data. However, in general we can still conclude that a warm AWP on interannual time scales tends to increase the precipitation in the central and eastern US and decrease the precipitation in the western US.

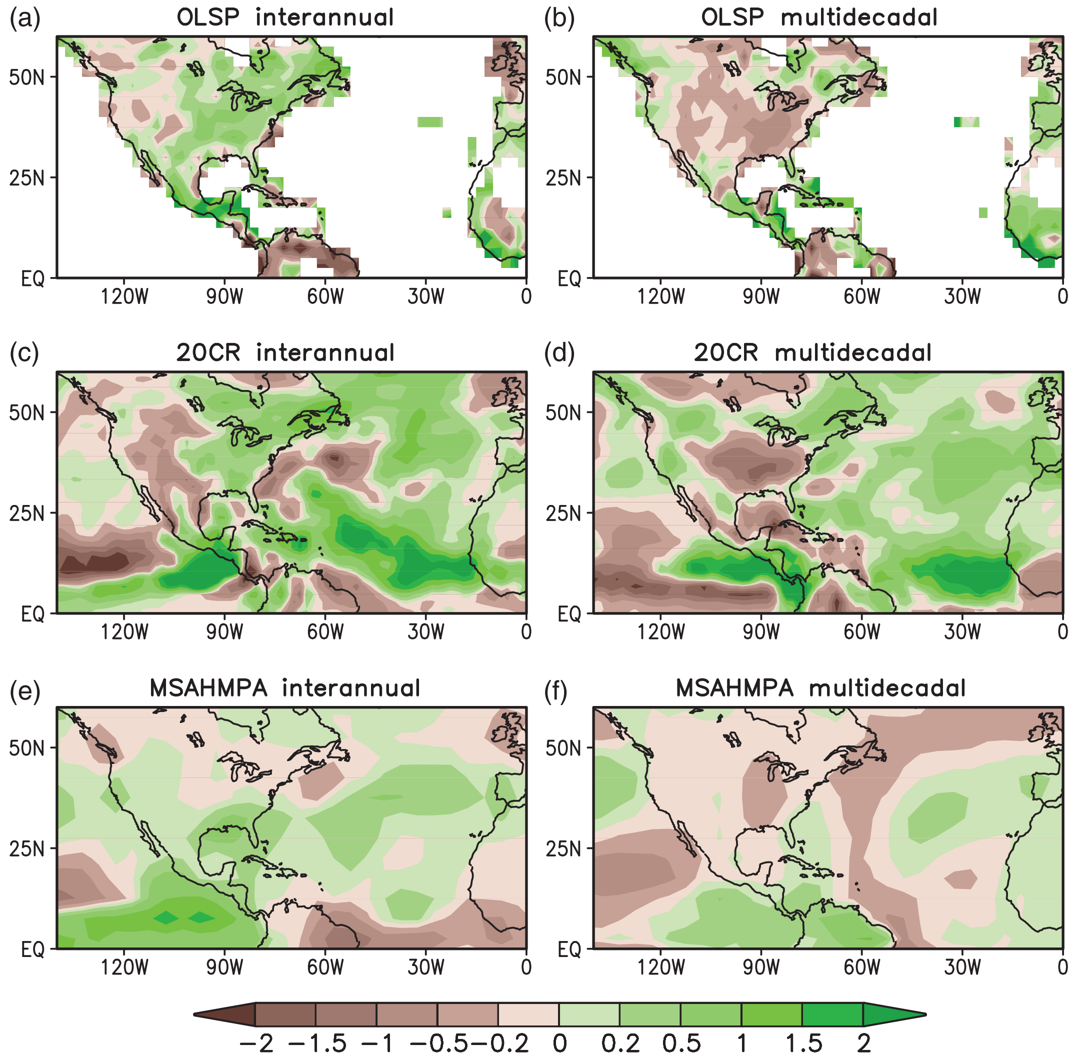

Figure 2. Regression of the precipitation data from (a) OLSP, (c) 20CR and (e) MSAHMPA onto interannual band AWPTI. Regression of the precipitation data from (b) OLSP, (d) 20CR and (f) MSAHMPA onto AWPTI of decadal-to-multidecadal band.

As shown in Figure 2(b) for OLSP station dataset, on decadal-to-multidecadal time scales a warm AWP tends to suppress the precipitation in the central and eastern US and enhance the precipitation in the western US. This feature is also well represented in Figure 2(d) based on the 20CR dataset and only roughly represented in Figure 2(f) based on the MSAHMPA dataset. Previous research has already shown that the dry response of US precipitation to the AWP on decadal-to-multidecadal time scales is the reflection of the impact of the AMO. Therefore, there is no surprise that the pattern of Figure 2(b)–(d) is identical with the pattern of AMO influence on US rainfall (Enfield *et al.*, 2001; Kushnir *et al.*, 2010; Hu and Feng, 2012).

In summary, the warming of the AWP on interannual time scales is associated with the tripole SST pattern which leads to more precipitation in the central and eastern US and less precipitation in the western US, while the warming of the AWP on the decadal-to-multidecadal time scales is associated with the warming pattern across the whole NA basin and leads to less precipitation in the central and eastern US. These two different precipitation patterns over the US continent are robust if we use the other precipitation datasets such as the high resolution precipitation data from the Climatic Research Unit (CRU) (Harris *et al.*, 2014) and extend the study period to 2013 (figures not shown).

4. A hypothesized physical mechanism

The mechanism for the AMO's influence on US precipitation has been addressed in previous studies (Kushnir *et al.*, 2010; Hu *et al.*, 2011; Nigam *et al.*, 2011). During the warm (cold) phase of the AMO, atmospheric circulation anomalies attenuate (enhance) moisture transport into the Great Plains and generate low-level subsidence (uplift), leading to less (more) rainfall in the central and eastern US (Wang *et al.*, 2006, 2008a; Kushnir *et al.*, 2010; Hu *et al.*, 2011; Nigam *et al.*, 2011). This process explains how the AWP on the longer time scale influences the US precipitation. The climatology of ASO moisture transport (Figure 3(a)) shows that the moisture is transported into the central

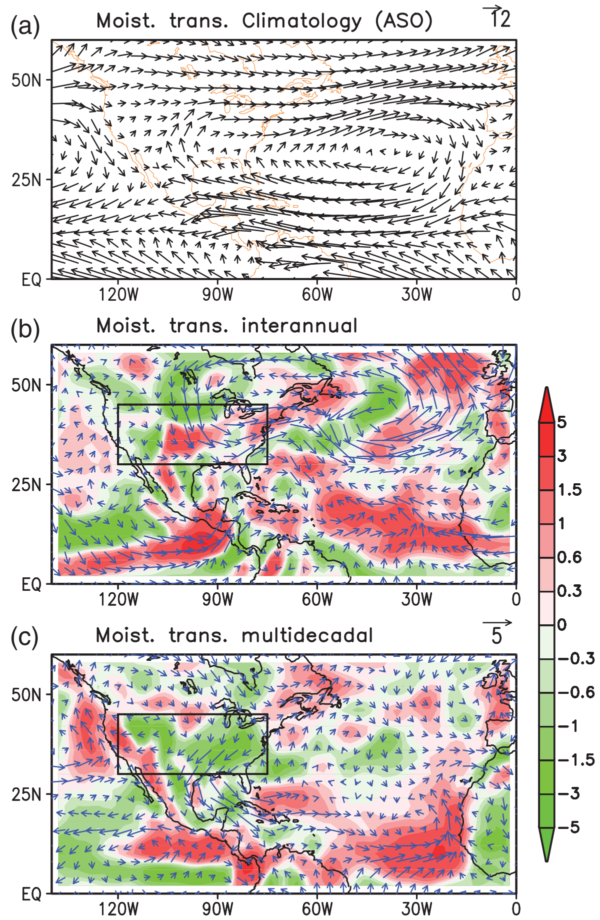

Figure 3. (a) The climatology of moisture transport in ASO integrated. Regression of moisture transport (vector) and moisture convergence (shading) onto (b) the interannual band AWPTI and (c) the decadal-to-multidecadal band AWPTI. Moisture transport (g kg^{-1} m s^{-1}) is calculated at each vertical level and integrated from sea surface to 300 mb. The unit of moisture convergence is 10^5 g kg^{-1} s^{-1}.

and eastern US in late summer and early fall through the Carribean Low-Level Jet (CLLJ) and the Great Plains Low-Level Jet (GPLLJ) (Wang *et al.*, 2007, 2008a). As shown in Figure 3(c), a warm AWP weakens the moisture transport of the GPLLJ and also the CLLJ. Over the North American continent between 20° and 60°N, an anticyclonic pattern of moisture transport is formed, which leads to the moisture divergence across the central and eastern US and moisture convergence in the western US. This pattern explains well the precipitation pattern corresponding to the DMB AWPTI shown in Figure 2(d).

However, the processes of moisture transport described above differ from the processes for the precipitation impact of the AWP on interannual time scales. As shown in Figure 3(b), a warm AWP does decrease the northward GPLLJ moisture transport but to some extent increases the moisture transport in the Gulf of Mexico region. Between 30° and 60°N to the east of 110°W a cyclonic moisture transport is formed, which results in the moisture convergence in the most regions of the central and eastern US and moisture divergence to the west of 110°W. This pattern is also consistent with the precipitation pattern associated with IB AWPTI as shown in Figure 2(c).

Why does a warm AWP cause two different moisture transport patterns on the different time scales? We argue that the two different NA SST patterns associated with a warm AWP on the IB and DMB time scales are the dominant factors. The SLP and HGT at 500 mb are regressed on DMB AWPTI (Figure 4(b) and (d)) and the patterns are generally consistent with the three-cell anomalous atmospheric circulation discussed in Hu *et al.* (2011) for explaining the decreased GPLLJ and CLLJ.

Compared with the pressure patterns of Figure 4(b) and (d), the major difference for the AWP impact on interannual time scales is the enhanced barotropic response located from 40° to 55°N and 90° to 60°W over the northeastern part of North America and extending to the NA (Figure 4(a) and (c)). The low SLP center over the northeastern North American continent (Figure 4(a)) is excited by the ASO heating over the continent and enhanced by the temperature contrast between the land and the ocean near the location of the negative SST node of the tripole pattern shown in Figure 1(f). Furthermore, the Gill-type response (Gill, 1980) over the AWP region is propagated in the form of a barotropic Rossby wave (Lee *et al.,* 2009) to the high latitude and results in the barotropic response over the continental region within 40°–55°N. It is the anomalous low pressure system over northeastern part of the North American continent that leads to the cyclonic moisture transport pattern in Figure 3(b) and thus results in the precipitation pattern shown in Figure 2(c). This low pressure system does not exist for the scenario of the AWP impact on decadal-to-multidecadal time scales in which a uniform (non-tripole) warming occurs over the entire NA and lacks a negative node in the mid-latitudes.

On the basis of the two NA SST patterns of ASO associated with IB AWPTI and DMB AWPTI and the discussion above, we suggest that the contrasting mid-latitude SSTs of the NA influence US precipitation through different atmospheric circulation responses: The sign of mid-latitude SST anomaly associated with the AWP warming determines two almost opposite precipitation patterns over the US. The underlying physical mechanism of how the mid-latitude SSTs influence the mid-latitude air–sea interaction and atmospheric circulation is still not understood.

5. Conclusions and discussion

Previous studies have shown that the AMO plays a fundamental role in US precipitation on decadal and multidecadal time scales and the climate response to the basin-wide AMO SST anomalies is primarily forced by the tropical Atlantic SST anomalies. The role of the sign of mid-latitude SST anomaly in the US precipitation associated with the warming of the TNA has not been emphasized. In this study, we examine the AWP variability in ASO and show that the warming of the AWP

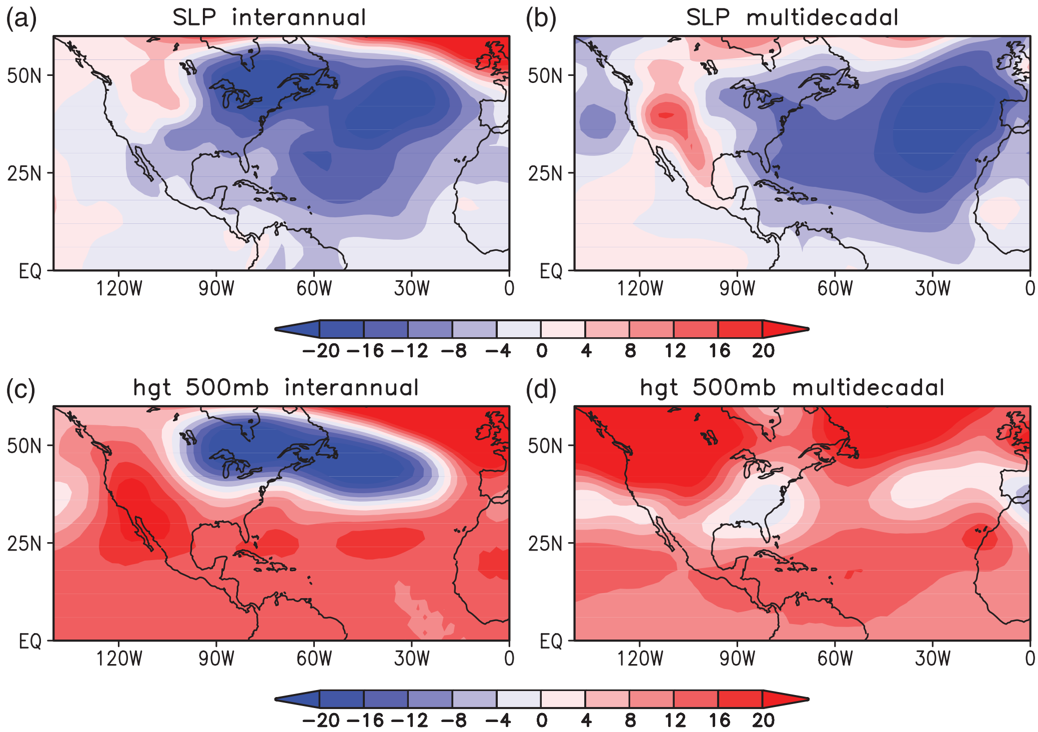

Figure 4. Regression of ASO SLP (Pa) onto (a) interannual band AWPTI and (b) decadal-to-multidecadal band AWPTI. Regression of ASO geopotential height (m) at 500 mb onto (c) interannual band AWPTI and (d) decadal-to-multidecadal band AWPTI.

on interannual time scales corresponds to a tripole SST pattern in the NA. This pattern leads to an anomalous high pressure system over the northeastern North American continent and results in more precipitation over the central and eastern US and less precipitation in the western US through the associated moisture transport over the US. On decadal and multidecadal time scales, the warming of the AWP is associated with a basin-wide SST warming pattern in the NA, i.e. AMO SST pattern. Through the induced variation of moisture transport, the warming SST pattern across the basin leads to less precipitation in the central and eastern US and more precipitation in the western US.

Comparing the two SST patterns associated with the warming of the AWP, we conclude that the mid-latitude SST variation does exert an influence on the US precipitation. A hypothesis is proposed that the mid-latitude negative SST anomaly center of the tripole SST pattern discussed above enhances the low SLP center over the northeastern North American continent caused by ASO land heating through land–ocean temperature contrast. This mid-latitude negative SST anomaly also enhances the local barotropic response of the barotropic Rossby wave excited by the AWP warming and propagated from the tropical region. On decadal-to-multidecadal time scales, the mid-latitude SST anomaly exhibits the positive sign associated with the AWP warming and the low pressure system over the northeastern North American continent is not produced. It is the low pressure system that directly makes the difference on US precipitation. As discussed in Sutton and Hodson (2007), the response to the tropical and mid-latitude SST anomalies is a nonlinear interaction and the mechanism for this nonlinearity is still not clear. Further investigation is needed to understand the role of mid-latitude SST.

As the combination of the opposite impacts of the AWP on interannual time scales and decadal-to-multidecadal time scales dominates the influence of the AWP on the US precipitation, the findings of this study provide another view to understand the extreme events or mitigation in certain years under a long term drought background.

Acknowledgements

We thank two reviewers for their comments on the manuscript. This work was supported by grants from National Oceanic and Atmospheric Administration (NOAA) Climate Program Office and the base funding of NOAA Atlantic Oceanographic and Meteorological Laboratory (AOML). The findings and conclusions in this report are those of the author(s) and do not necessarily represent the views of the funding agency.

References

Compo GP, Whitaker JS, Sardeshmukh PD, Matsui N, Allan RJ, Yin X, Gleason BE, Vose RS, Rutledge G, Bessemoulin P, Brönnimann S, Brunet M, Crouthamel RI, Grant AN, Groisman PY, Jones PD, Kruk MC, Kruger AC, Marshall GJ, Maugeri M, Mok HY, Nordli O, Ross TF, Trigo RM, Wang XL, Woodruff SD, Worley SJ. 2011. The twentieth century reanalysis project. *Quarterly Journal of the Royal Meteorological Society* **137**: 1–28.

Dai A. 2013. The influence of the inter-decadal Pacific oscillation on US precipitation during 1923–2010. *Climate Dynamics* **41**: 633–646.

Dai A, Fung IY, Del Genio AD. 1997. Surface observed global land precipitation variations during 1900–1988. *Journal of Climate* **10**: 2943–2962.

Enfield DB, Mestas-Nuñez AM, Trimble PJ. 2001. The Atlantic Multidecadal Oscillation and its relation to rainfall and river flows in the continental US. *Geophysical Research Letters* **28**: 2077–2080.

Fan M, Schneider E. 2012. Observed decadal North Atlantic tripole SST variability. Part I: Weather noise forcing and coupled response. *Journal of the Atmospheric Sciences* **69**(1): 35–50.

Gill AE. 1980. Some simple solutions for heat-induced tropical circulation. *Quarterly Journal of the Royal Meteorological Society* **106**: 447–462.

Harris I, Jones PD, Osborn TJ, Lister DH. 2014. Updated high-resolution grids of monthly climatic observations – the CRU TS3.10 Dataset. *International Journal of Climatology* **34**: 623–642, doi: 10.1002/joc.3711.

Hu Q, Feng S. 2012. AMO- and ENSO-driven summertime circulation and precipitation variations in North America. *Journal of Climate* **25**: 6477–6495.

Hu Q, Feng S, Oglesby RJ. 2011. Variations in North American summer precipitation driven by the Atlantic Multidecadal Oscillation. *Journal of Climate* **24**(21): 5555–5570.

Kushnir Y. 1994. Interdecadal variations in North Atlantic sea surface temperature and associated atmospheric conditions. *Journal of Climate* **7**: 141–157.

Kushnir Y, Robinson WA, Bladé I, Hall NMJ, Peng S, Sutton R. 2002. Atmospheric GCM response to extratropical SST anomalies: synthesis and evaluation. *Journal of Climate* **15**: 2233–2256.

Kushnir Y, Seager R, Ting M, Naik N, Nakamura J. 2010. Mechanisms of tropical Atlantic SST influence on North American precipitation variability. *Journal of Climate* **23**: 5610–5628.

Lee S-K, Wang C, Mapes BE. 2009. A simple atmospheric model of the local and teleconnection responses to tropical heating anomalies. *Journal of Climate* **22**: 272–284.

Li L, Li W, Kushnir Y. 2011. Variation of North Atlantic subtropical high western ridge and its implication to the Southeastern US summer precipitation. *Climate Dynamics* **39**: 1401–1412.

Liu H, Wang C, Lee S-K, Enfield D. 2012. Atlantic warm-pool variability in the IPCC AR4 CGCM simulations. *Journal of Climate* **25**: 5612–5628.

Mantua NJ, Steven RH, Zhang Y, Wallace JM, Francis RC. 1997. A pacific interdecadal climate oscillation with impacts on salmon production. *Bulletin of the American Meteorological Society* **78**: 1069–1079.

McCabe GJ, Palecki MA, Betancourt JL. 2004. Pacific and Atlantic Ocean influences on multidecadal drought frequency in the United States. *Proceedings of the National Academy of Sciences of the United States of America* **101**: 4136–4141.

Mestas-Nunez A, Enfield DB. 1999. Rotated global modes of non-ENSO sea surface temperature variability. *Journal of Climate* **12**: 2734–2746.

Mo KC, Paegle JN, Paegle J. 1995. Physical mechanisms of the 1993 summer floods. *Journal of the Atmospheric Sciences* **52**: 879–895.

Mo KC, Schemm JE, Yoo S-H. 2009. Influence of ENSO and the Atlantic Multidecadal Oscillation on drought over the United States. *Journal of Climate* **22**: 5962–5982.

Nigam S, Guan B, Ruiz-Barradas A. 2011. Key role of the Atlantic Multidecadal Oscillation in 20th century drought and wet periods over the Great Plains. *Geophysical Research Letters* **38**: L16713.

Palmer TN, Sun Z. 1985. A modelling and observational study of the relationship between sea surface temperature in the North-West Atlantic and the atmospheric general circulation. *Quarterly Journal of the Royal Meteorological Society* **111**(470): 947–975.

Peng S, Whitaker JS. 1999. Mechanisms determining the atmospheric response to midlatitude SST anomalies. *Journal of Climate* **12**: 1393–1408.

Ropelewski CF, Halpert MS. 1986. North American precipitation and temperature patterns associated with the El Nino–Southern Oscillation (ENSO). *Monthly Weather Review* **114**: 2352–2362.

Ruiz-Barradas A, Nigam S. 2010. Great Plains precipitation and its SST links in 20th century climate simulations, and 21st and 22nd century climate projections. *Journal of Climate* **23**: 6409–6429.

Schubert SD, Suarez MJ, Pegion PJ, Koster RD, Bacmeister JT. 2004a. Causes of long-term drought in the US Great Plains. *Journal of Climate* **17**: 485–503.

Schubert SD, Suarez MJ, Pegion PJ, Koster RD, Bacmeister JT. 2004b. On the cause of the 1930s Dust Bowl. *Science* **303**: 1855–1859.

Seager R, Kushnir Y, Herweijer C, Naik N, Velez J. 2005. Modeling of tropical forcing of persistent droughts and pluvials over western North America: 1856–2000. *Journal of Climate* **18**: 4068–4091.

Smith TM, Reynolds RW, Peterson TC, Lawrimore J. 2008. Improvements NOAAs Historical Merged Land–Ocean Temp Analysis (1880–2006). *Journal of Climate* **21**: 2283–2296.

Smith TM, Arkin PA, Sapiano MRP, Chang C. 2010. Merged statistical analyses of historical monthly precipitation anomalies beginning 1900. *Journal of Climate* **23**: 5755–5770.

Sutton RT, Hodson DLR. 2005. Atlantic Ocean forcing of North American and European summer climate. *Science* **309**: 115–118.

Sutton RT, Hodson DLR. 2007. Climate response to basin-scale warming and cooling of the North Atlantic Ocean. *Journal of Climate* **20**: 891–907.

Ting M, Wang H. 1997. Summertime US precipitation variability and its relation to Pacific sea surface temperature. *Journal of Climate* **10**: 1853–1873.

Trenberth KE, Guillemot VJ. 1996. Physical processes in 1988 drought and 1993 floods in North America. *Journal of Climate* **9**: 1288–1298.

Veres MC, Hu Q. 2013. AMO-forced regional processes affecting summertime precipitation variations in the Central United States. *Journal of Climate* **26**: 276–290.

Wang C, Enfield DB. 2001. The tropical Western Hemisphere warm pool. *Geophysical Research Letters* **28**: 1635–1638, doi: 10.1029/2000GL011763.

Wang C, Enfield DB, Lee S-K, Landsea CW. 2006. Influences of the Atlantic warm pool on Western Hemisphere summer rainfall and Atlantic hurricanes. *Journal of Climate* **19**: 3011–3028.

Wang C, Lee S, Enfield DB. 2007. Impact of the Atlantic warm pool on the summer climate of the Western Hemisphere. *Journal of Climate* **20**: 5021–5040.

Wang C, Lee S-K, Enfield DB. 2008a. Climate response to anomalously large and small Atlantic warm pools during the summer. *Journal of Climate* **21**: 2437–2450.

Wang C, Lee S-K, Enfield DB. 2008b. Atlantic warm pool acting as a link between Atlantic multidecadal oscillation and Atlantic tropical cyclone activity. *Geochemistry, Geophysics, Geosystems* **9**: Q05V03, doi: 10.1029/2007GC001809.

Zhu J, Huang B, Hu Z, Kinter J, Marx L. 2013. Predicting US summer precipitation using NCEP Climate Forecast System version 2 initialized by multiple ocean analyses. *Climate Dynamics* **41**(7–8): 1941–1954.

